Int. J. Heat Mass Transfer. Vol. 36, No. 6, pp. 1573–1582, 1993
Printed in Great Britain

0017-9310/93 $6.00 + 0.00

Variable porosity effect on vortex instability of a horizontal mixed convection flow in a saturated porous medium

JIIN-YUH JANG and JIING-LIN CHEN
Department of Mechanical Engineering, National Cheng-Kung University, Tainan, Taiwan 70101, R.O.C.

(*Received* 8 *May* 1992 *and in final form* 26 *June* 1992)

Abstract—A numerical analysis is made to analyze the variable porosity effect on the vortex mode of instability of a horizontal mixed convection boundary layer flow with a uniform free stream velocity in a saturated porous medium. The porosity of the medium is assumed to vary exponentially with distance from the wall. In the base flow, similarity solutions are obtained for the case of constant heat flux boundary condition. The stability analysis is based on the linear stability theory and the resulting eigenvalue problem is solved by the local similarity method. It is found that the variable porosity effect tends to increase the heat transfer rate and destabilize the flow to the vortex mode of disturbance. The effects of fluid–solid thermal conductivity ratio on the heat transfer and vortex instability are more significant for a uniform porosity medium than for a variable porosity medium.

1. INTRODUCTION

THE PROBLEMS of vortex mode of instability in natural or mixed convection flow over a heated plate in a saturated porous medium have recently received considerable attention. This is primarily due to a large number of technical applications, such as fluid flow in geothermal reservoirs, separation processes in chemical industries, storage of radioactive nuclear waste materials, transpiration cooling, transport processes in aquifers, etc. The instability mechanism is due to the presence of a buoyancy force component in the direction normal to the plate surface.

For natural convection boundary layer flow adjacent to a flat plate, Hsu *et al.* [1] and Hsu and Cheng [2] analyzed the vortex mode of instability of horizontal and inclined natural convection flows in a uniform porosity medium. Jang and Chang [3] re-examined the same problem for an inclined plate, where both the streamwise and normal components of the buoyancy force are retained in the momentum equations. Jang and Chang [4] studied the vortex instability of horizontal natural convection in a porous medium resulting from combined heat and mass buoyancy effects. The effects of a density extremum on the vortex instability of an inclined buoyant layer in porous media saturated with cold water were examined by Jang and Chang [5, 6].

For mixed convection boundary layer flow adjacent to a flat plate, Hsu and Cheng [7] analyzed the vortex instability for a horizontal mixed convection in a uniform porosity medium. By neglecting the normal component of buoyancy force, Cheng [8] showed that, in the main flow analysis, the mixed convection boundary layer flow over an inclined plate in a saturated porous medium can be approximated by the similarity solution for a vertical plate, with the gravity component parallel to the inclined plate incorporated in the Rayleigh number. Following the same approach, Hsu and Cheng [9] applied a linear stability analysis to determine the condition of onset of vortex instability for flow over an inclined surface. It is apparent that the instability results in ref. [9] are not valid for angles of inclination from the horizontal that are small. Thus, Jang and Lie [10] provided new vortex instability results for small angles of inclination from the horizontal ($\phi \leqslant 25^\circ$) and more accurate results for large angles of inclination ($\phi > 25^\circ$) than the previous study [9].

All of the works mentioned above are based on the Darcy formulation with uniform porosity. In some applications, such as fixed-bed catalytic reactors, packed bed heat exchangers and drying, the porosity is not uniform but has a maximum value at the wall and a minimum value away from the wall. This wall-channeling phenomenon has been reported by a number of investigators such as Vafai [11], Chandrasekhara *et al.* [12–14] and Hong *et al.* [15] for forced, natural or mixed convection boundary layer flows adjacent to a horizontal or vertical plate. It is shown that the variable porosity effect increases the temperature gradient adjacent to the wall resulting in the enhancement of surface heat flux. However, the variable porosity effect on the *vortex instability* of a horizontal mixed convection boundary layer flow in a porous medium does not seem to have been investigated. This has motivated the present investigation.

The purpose of this paper is to examine the variable porosity effect on the vortex instability of a horizontal mixed convection flow in a porous medium. The vari-

NOMENCLATURE

A	constant on the wall temperature relation
a	dimensional spanwise wave number
d	constant defined by equation (8)
d^*	constant defined by equation (9)
f	similarity stream function profile
F	dimensionless disturbance stream function amplitude, $\tilde{\psi}/i\alpha_x Ra_x^{1/3}$
g	gravitational acceleration
h	local heat transfer coefficient
$\tilde{k}$	dimensionless wave number, $ax/Ra_x^{1/3}$
K	permeability of the porous medium
m	exponent on wall temperature relation
Nu_x	local Nusselt number, hx/λ_f
p	pressure
p'	perturbation pressure
Pe_x	local Peclet number, $U_\infty x/\alpha_x$
q''	local heat flux
Ra_x	modified local Rayleigh number, $K_x g\beta(T_w-T_\infty)/\alpha_x \nu$
T	temperature
T'	perturbation temperature
$\tilde{T}$	disturbance temperature amplitude
$\tilde{u}$	x direction disturbance velocity amplitude
u, v, w	volume averaged velocity in the x, y, z directions
u', v', w'	disturbance velocity in the x, y, z directions
x, y, z	axial, normal and spanwise coordinates.

Greek symbols

α	effective thermal diffusivity of the porous medium
β	coefficient of the fluid thermal expansion
γ	coefficient defined by equation (8)
ε	porosity
η	similarity variable, $(y/x)Ra_x^{1/3}$
Θ	dimensionless disturbance temperature amplitude
θ	dimensionless temperature, $(T-T_\infty)/(T_w-T_\infty)$
λ_f, λ_s	thermal conductivities of the fluid and solid phases
λ_m	effective thermal conductivity of the porous medium
μ	absolute viscosity
ξ	mixed convection parameter, $Pe_x^{3/2}/Ra_x$
ρ	density
ψ	stream function
ψ'	disturbance stream function
$\tilde{\psi}$	disturbance stream function amplitude.

Subscripts

w	condition at the wall
∞	condition at the free stream.

Superscript

*	critical condition.

able porosity is approximated by an exponential function. The non-Darcy effects, such as boundary, inertia and thermal dispersion effects on the vortex instability of a natural or mixed convection flow in a uniform porosity medium have been investigated by Chang and Jang [16, 17] and Jang and Chen [18]; these effects are neglected in the present study in order to obtain the similarity solution for the base flow [12, 13]. The analysis of the disturbance flow is based on linear stability theory. The disturbance quantities are assumed to be in the form of a stationary vortex roll that is periodic in the spanwise direction, with its amplitude function depending primarily on the normal coordinate and weakly on the streamwise coordinate. The resulting eigenvalue problem is solved using a variable step-size sixth-order Runge–Kutta integration scheme in conjunction with the Gram–Schmidt orthogonalization procedure [19] to maintain the linear independence of the eigenfunctions.

2. MATHEMATICAL FORMULATION

2.1. *The base flow*

Consider the problems of steady mixed convection in a semi-infinite porous medium bounded by a horizontal impermeable heated surface aligned parallel to a free stream with uniform velocity U_∞ and temperature T_∞ as shown in Fig. 1, where x represents the distance along the plate from its leading edge, and y the distance normal to the surface. The wall temperature is assumed to be a power function of x, i.e. $T_w = T_\infty + Ax^m$, where A and m are constants. If we assume that: (1) local thermal equilibrium exists between the fluid and solid phases, (2) the Boussinesq approximation is valid, (3) the porosity and effective thermal diffusivity of the porous medium are primarily functions of y coordinate [11, 15], then the governing equations in a variable porosity medium

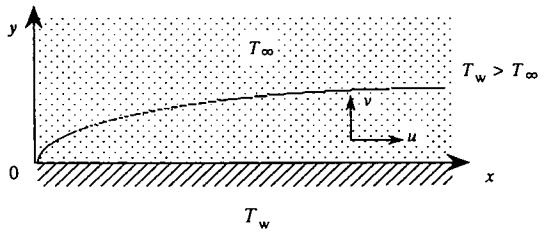

FIG. 1. The physical model and coordinate system.

based on Darcy's law are given by

$$\frac{\partial u}{\partial x}+\frac{\partial v}{\partial y}=0 \tag{1}$$

$$u=-\frac{K(y)}{\mu}\frac{\partial p}{\partial x} \tag{2}$$

$$v=-\frac{K(y)}{\mu}\left[\frac{\partial p}{\partial y}-\rho g\beta(T-T_\infty)\right] \tag{3}$$

$$u\frac{\partial T}{\partial x}+v\frac{\partial T}{\partial y}=\alpha(y)\frac{\partial^2 T}{\partial x^2}+\frac{\partial}{\partial y}\left(\alpha(y)\frac{\partial T}{\partial y}\right) \tag{4}$$

where $K(y)$ is the permeability of the porous medium; β the thermal expansion coefficient of the fluid; $\alpha(y)=\lambda_m(y)/(\rho_\infty c_p)_f$ the effective thermal diffusivity of the porous medium ($\lambda_m(y)$ denotes the effective thermal conductivity of the saturated porous medium and $(\rho_\infty c_p)_f$ denotes the product of density and specific heat of the fluid). The other symbols are defined in the Nomenclature.

The pressure terms appearing in equations (2) and (3) can be eliminated through cross differentiation. By applying the boundary-layer assumptions and introducing the stream function ψ which automatically satisfies equation (1), equations (1)–(4) become

$$\frac{\partial^2\psi}{\partial y^2}=-K(y)\frac{\partial}{\partial y}\left[\frac{1}{K(y)}\right]\frac{\partial\psi}{\partial y}-\frac{K(y)\rho g\beta}{\mu}\frac{\partial T}{\partial x} \tag{5}$$

$$\frac{\partial\psi}{\partial y}\frac{\partial T}{\partial x}-\frac{\partial\psi}{\partial x}\frac{\partial T}{\partial y}=\alpha(y)\frac{\partial^2 T}{\partial y^2}+\frac{\partial\alpha(y)}{\partial y}\frac{\partial T}{\partial y}. \tag{6}$$

The boundary conditions for this problem are

$$\text{at}\quad y=0,\quad v=-\frac{\partial\psi}{\partial x}=0,\quad T_w=T_\infty+Ax^m$$

$$y\to\infty,\quad T=T_\infty,\quad u=\frac{\partial\psi}{\partial y}=0,\quad \text{for free convection}$$

$$u=\frac{\partial\psi}{\partial y}=u_\infty,\quad \text{for mixed convection.} \tag{7}$$

Here we assume that the porosity $\varepsilon(y)$ and permeability $K(y)$ vary exponentially from the wall [12, 13]

$$\varepsilon(y)=\varepsilon_\infty(1+d\,e^{-y/\gamma}) \tag{8}$$

$$K(y)=K_\infty(1+d^*\,e^{-y/\gamma}) \tag{9}$$

where ε_∞ and K_∞ are the porosity and permeability at the edge of the boundary layer; d and d^* are constants whose values are taken as 1.5 and 3, respectively [12, 13]. Further, $\alpha(y)=\lambda_m(y)/(\rho_\infty c_p)_f$ also varies from the wall since it is related to the effective thermal conductivity of the saturated porous medium $\lambda_m(y)$. $\lambda_m(y)$ can be computed according to the following semi-analytical expression given by Zehner and Schlünder [20]:

$$\frac{\lambda_m}{\lambda_f}=1-\sqrt{(1-\varepsilon)}+\frac{2\sqrt{(1-\varepsilon)}}{1-\sigma B}\left[\frac{(1-\sigma)B}{(1-\sigma B)^2}\ln\left(\frac{1}{\sigma B}\right)-\frac{B+1}{2}-\frac{B-1}{1-\sigma B}\right] \tag{10a}$$

where λ_f is the thermal conductivity of the fluid phase, $\sigma=\lambda_f/\lambda_s$ the fluid–solid thermal conductivity ratio and $B=1.25\,((1-\varepsilon)/\varepsilon)^{10/9}$ for a packed sphere bed.

Hence the expression for the effective thermal diffusivity has the form

$$\frac{\alpha(y)}{\alpha_\infty}=1-(1-\varepsilon_\infty(1+d\,e^{-y/\gamma}))^{1/2}+\frac{2(1-\varepsilon_\infty(1+d\,e^{-y/\gamma}))^{1/2}}{1-\sigma B}\cdot\left[\frac{(1-\sigma)B}{(1-\sigma B)^2}\ln\left(\frac{1}{\sigma B}\right)-\frac{B+1}{2}-\frac{B-1}{1-\sigma B}\right] \tag{10b}$$

where $\alpha_\infty=k_f/(\rho_\infty c_p)_f$. On introducing the following dimensionless similarity variables [12]:

$$\eta=Ra_x^{1/3}\frac{y}{x},\quad f(\eta)=\frac{\psi}{\alpha_\infty Ra_x^{1/3}},\quad \theta(\eta)=\frac{T-T_\infty}{T_w-T_\infty} \tag{11}$$

where $Ra_x=K_\infty g\beta(T_w-T_\infty)_x/\alpha_\infty\nu$ is the modified local Rayleigh number, and choosing $\gamma=x/Ra_x^{1/3}$ such that $K(y)$ and $\varepsilon(y)$ are purely functions of η for the sake of similarity solutions can be justified [12, 13].

Equations (5) and (6) can be nondimensionalized as follows:

$$f'''+\frac{d^*\,e^{-\eta}}{1+d^*\,e^{-\eta}}f'+m(1+d^*\,e^{-\eta})\theta+\frac{m-2}{3}(1+d^*\,e^{-\eta})\eta\theta'=0 \tag{12}$$

$$\frac{\alpha(\eta)}{\alpha_\infty}\theta''=mf'\theta-\frac{m+1}{3}f\theta'-\frac{d}{d\eta}\left[\frac{\alpha(\eta)}{\alpha_\infty}\right]\theta'. \tag{13}$$

The corresponding boundary conditions are

$$f(0)=0,\quad \theta(0)=1,\quad \theta(\infty)=0$$

$$f'(\infty)=0,\quad \text{natural convection}$$

$$f'(\infty)=\frac{U_\infty}{\alpha_\infty}\left(\frac{\nu\alpha_\infty}{K_\infty g\beta A}\right)^{2/3}x^{(1-2m)/3},$$

$$\text{mixed convection.} \tag{14}$$

From boundary condition (14), it can be seen that the similarity solutions exist only if $m=0.5$ (i.e. constant heat flux). Then equations (12) and (13) become

$$f''+\frac{d^*\,e^{-\eta}}{1+d^*\,e^{-\eta}}f'+\tfrac{1}{2}(1+d^*\,e^{-\eta})\theta -\tfrac{1}{2}(1+d^*\,e^{-\eta})\eta\theta'=0 \quad (15)$$

$$\frac{\alpha(\eta)}{\alpha_\infty}\theta''=\tfrac{1}{2}f'\theta-\tfrac{1}{2}f\theta'-\frac{d}{d\eta}\left[\frac{\alpha(\eta)}{\alpha_\infty}\right]\theta' \quad (16)$$

with boundary conditions

$$\eta=0,\quad \theta=1,\quad f=0$$
$$\eta\to\infty,\quad \theta=0,\quad f'=0,\quad \text{for natural convection}$$
$$f'=\xi,\quad \text{for mixed convection} \quad (17)$$

where

$\xi = Pe_x^{3/2}/Ra_x$, mixed convection parameter

$Pe_x = u_\infty x/\alpha_\infty$, local Peclet number.

It is noted that ξ is the mixed convection parameter, which measures the relative importance of forced to free convection; $\xi = 0$ corresponds to the case of purely free convection. As $d = d^* = 0$, equations (15)–(17) reduce to Darcy's model with uniform porosity [1, 7].

In terms of the dimensionless variables, it can be shown that the velocities and local Nusselt number are given by

$$u=\frac{\alpha_\infty Ra_x^{2/3}}{x}f' \quad (18)$$

$$v=-\alpha_\infty\left(\frac{K_\infty g\beta A}{\nu\alpha_\infty}\right)^{1/3}[\tfrac{1}{2}f-\tfrac{1}{2}\eta f']x^{-1/2} \quad (19)$$

$$Nu_x=\frac{hx}{\lambda_f}=\frac{q''(x)x}{\lambda_f(T_w-T_\infty)}=\frac{\lambda_m(0)}{\lambda_f}Ra_x^{1/3}[-\theta'(0)]. \quad (20)$$

2.2. *The disturbance flow*

The standard method of linear stability theory is that in which the instantaneous values of the velocity, pressure and temperature are perturbed by small amplitude disturbances and the base flow equations are subtracted, with terms higher than first order in disturbance quantities being neglected. Then we get the following disturbance equations for a variable porosity medium:

$$\frac{\partial u'}{\partial x}+\frac{\partial v'}{\partial y}+\frac{\partial w'}{\partial z}=0 \quad (21)$$

$$u'=-\frac{K(y)}{\mu}\frac{\partial p'}{\partial x} \quad (22)$$

$$v'=-\frac{K(y)}{\mu}\left(\frac{\partial p'}{\partial y}-\rho g\beta T'\right) \quad (23)$$

$$w'=-\frac{K(y)}{\mu}\frac{\partial p'}{\partial z} \quad (24)$$

$$\bar u\frac{\partial T'}{\partial x}+\bar v\frac{\partial T'}{\partial y}+u'\frac{\partial\bar T}{\partial x}+v'\frac{\partial\bar T}{\partial y}=\alpha(y)\frac{\partial^2 T'}{\partial x^2}+\frac{\partial}{\partial y}\left[\alpha(y)\frac{\partial T'}{\partial y}\right]+\alpha(y)\frac{\partial^2 T'}{\partial z^2} \quad (25)$$

where the barred and primed quantities signify the base flow and disturbance components, respectively.

Following the method of order-of-magnitude analysis described in detail by Hsu and Cheng [2], the terms $\partial u'/\partial x$, $\partial^2 T'/\partial x^2$ in equations (21) and (25) can be neglected. The omission of $\partial u'/\partial x$ in equation (21) implies the existence of a disturbance stream function ψ' such that

$$v'=-\frac{\partial\psi'}{\partial z},\quad w'=\frac{\partial\psi'}{\partial y}. \quad (26)$$

We assume that the three-dimensional disturbances are of the form

$$(\psi',u',T')=[\tilde\psi(x,y),\tilde u(x,y),\tilde T(x,y)]\exp(iaz+q(x)) \quad (27)$$

where a is the spanwise periodic wave number, and $q(x)=\int\omega(x)\,dx$.

With $\omega(x)$ denoting the spatial growth factor. For the lowest order approximation $q(x)=\omega x$. Setting $\omega=0$ for neutral stability yields

$$ia\tilde u=\frac{\partial^2\tilde\psi}{\partial x\,\partial y} \quad (28)$$

$$\frac{\partial^2\tilde\psi}{\partial y^2}-a^2\tilde\psi=\frac{1}{K(y)}\frac{\partial K(y)}{\partial y}\frac{\partial\tilde\psi}{\partial y}-\frac{iaK(y)\rho g\beta}{\mu}\tilde T \quad (29)$$

$$\frac{\partial\alpha(y)}{\partial y}\frac{\partial\tilde T}{\partial y}+\alpha(y)\frac{\partial^2\tilde T}{\partial y^2}-\alpha(y)a^2\tilde T=\bar u\frac{\partial\tilde T}{\partial x}+\bar v\frac{\partial\tilde T}{\partial y}+\tilde u\frac{\partial\bar T}{\partial x}-ia\tilde\psi\frac{\partial\bar T}{\partial y}. \quad (30)$$

Equations (28)–(30) are solved based on the local similarity approximations [2], wherein the disturbances are assumed to have weak dependence in the streamwise direction (i.e. $\partial/\partial x \ll \partial/\partial\eta$). Introducing the following dimensionless quantities:

$$\tilde k=\frac{ax}{Ra_x^{1/3}},\quad F(\eta)=\frac{\tilde\psi}{i\alpha_\infty Ra_x^{1/3}},\quad \Theta(\eta)=\frac{\tilde T}{T_w-T_\infty} \quad (31)$$

we obtain the following system of equations for the local similarity approximations:

$$F''+\frac{d^*\,e^{-\eta}}{1+d^*\,e^{-\eta}}F'-\tilde k^2F=-(1+d^*\,e^{-\eta})Ra_x^{1/3}\tilde k\Theta \quad (32)$$

$$\frac{\alpha(\eta)}{\alpha_\infty}\Theta'' + \left\{\frac{\partial}{\partial\eta}\left[\frac{\alpha(\eta)}{\alpha_\infty}\right] + \tfrac{1}{2}f\right\}\Theta' - \left\{\frac{\alpha(\eta)}{\alpha_\infty}\tilde{k}^2 + \tfrac{1}{2}f'\right\}\Theta = \frac{1}{4\tilde{k}\,Ra_x^{1/3}}(\eta\theta' - \theta)\eta F'' + \tilde{k}\,Ra_x^{1/3}\,\theta' F \quad (33)$$

with the boundary conditions

$$F(0) = \Theta(0) = F(\infty) = \Theta(\infty) = 0 \quad (34)$$

where the primes indicate the derivatives with respect to η. Equation (34) arises from the fact that the disturbances vanish at the wall and in the free stream in the porous medium. Equations (32) and (33) constitute a fourth-order system of linear ordinary differential equations for the disturbance amplitude distribution $F(\eta)$ and $\Theta(\eta)$. For fixed σ, ε_∞, d, d^*, and ξ, the solutions F and Θ are eigenfunctions for the eigenvalues Ra_x and $\tilde{k}$. For the case of $d = d^* = 0$, the equations reduce to the conventional disturbance equations for the uniform porosity assumption [1, 7].

3. NUMERICAL METHOD OF SOLUTION

In the stability calculations, the disturbance equations are solved by separately integrating two linearly independent integrals. The full solution may be written as the sum of two linearly independent solutions

$$F(\eta) = F_1(\eta) + EF_2(\eta) \quad (35)$$

$$\Theta(\eta) = \Theta_1(\eta) + E\Theta_2(\eta). \quad (36)$$

The two independent integrals (F_i, Θ_i), with $i = 1, 2$, may be chosen so that their asymptotic solutions are

$$F_1(\eta_\infty) = N\exp(\Gamma\eta_\infty), \quad F_2(\eta_\infty) = \exp(\Lambda\eta_\infty) \quad (37)$$

$$\Theta_1(\eta_\infty) = \exp(\Gamma\eta_\infty), \quad \Theta_2(\eta_\infty) = 0 \quad (38)$$

where

$$N = -\frac{(1+d^*\,e^{-\eta})\tilde{k}\,Ra_x^{1/3}}{\Gamma^2 + \dfrac{d^*\,e^{-\eta}}{1+d^*\,e^{-\eta}}\Gamma - \tilde{k}^2}$$

$$\Gamma = -\frac{\Omega + \left\{\Omega^2 + 4\dfrac{\alpha(\eta)}{\alpha_\infty}\left[\dfrac{\alpha(\eta)}{\alpha_\infty}\tilde{k}^2 + \tfrac{1}{2}f'\right]\right\}^{1/2}}{2\dfrac{\alpha(\eta)}{\alpha_\infty}}$$

$$\Lambda = -\frac{d^*\,e^{-\eta}}{2(1+d^*\,e^{-\eta})} - \frac{1}{2}\left[\left(\frac{d^*\,e^{-\eta}}{1+d^*\,e^{-\eta}}\right)^2 + 4\tilde{k}^2\right]^{1/2}$$

$$\Omega = \frac{\partial}{\partial\eta}\left[\frac{\alpha(\eta)}{\alpha_\infty}\right] + \tfrac{1}{2}f.$$

A sixth-order variable step size Runge–Kutta integration routine is used here to solve first the base flow system, equations (15) and (16), and the results are stored for a fixed step size, $\Delta\eta = 0.02$, which is small enough to predict accurate linear interpolation between mesh points. Equations (32) and (33) with boundary conditions, equation (34), are then solved as follows. For specified σ, ε_∞, d, d^*, ξ, and $\tilde{k}$, Ra_x is guessed. Using equations (37) and (38) as starting values, the two integrals are integrated separately from the outer edge of the boundary layer to the wall using a sixth-order Runge–Kutta variable step size integrating routine incorporated with the Gram–Schmidt orthogonalization procedure [19] to maintain the linear independence of the eigenfunctions. The required input of the base flow to the disturbance equations is calculated, as necessary, by linear interpolation of the stored base flow. From the values of the integrals at the wall, E is determined using the boundary condition $\Theta(0) = 0$. A Taylor series expansion of the second boundary condition $F(0) = 0$ provides a correction scheme for the initial guess of Ra_x. Iterations continue until the second boundary condition is sufficiently close to zero ($< 10^{-6}$, typically).

4. RESULTS AND DISCUSSION

Numerical results for the tangential velocity, temperature profiles, Nusselt number, neutral stability curves, the critical Rayleigh number and wave number at the onset of vortex instability are presented for various values of mixed convection parameter ξ, in the range of 0–10 with ambient porosity $\varepsilon_\infty = 0.4$ and three different values of fluid–solid thermal conductivity ratio $\sigma = \lambda_f/\lambda_s = 0.2$ (air to asbestos), 1 (air to glass wool) and 5 (air to rock wool), respectively.

Figures 2 and 3 show simultaneously the velocity and temperature profiles across the boundary layer for the selected values of σ (0.2, 1 and 5) for $\xi = 0$ (purely free convection) and for $\xi = 1$ (mixed convection), respectively. The velocity profiles are

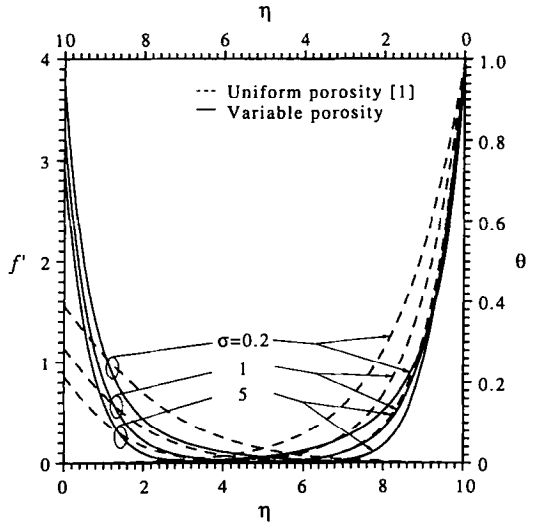

FIG. 2. Tangential velocity and temperature profiles across the boundary layer for selected values of σ for $\xi = 0$ (purely free convection).

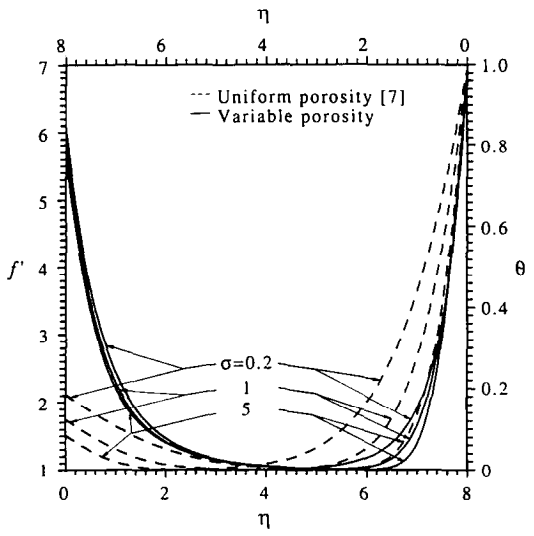

FIG. 3. Tangential velocity and temperature profiles across the boundary layer for selected values of σ for $\xi = 1$ (mixed convection).

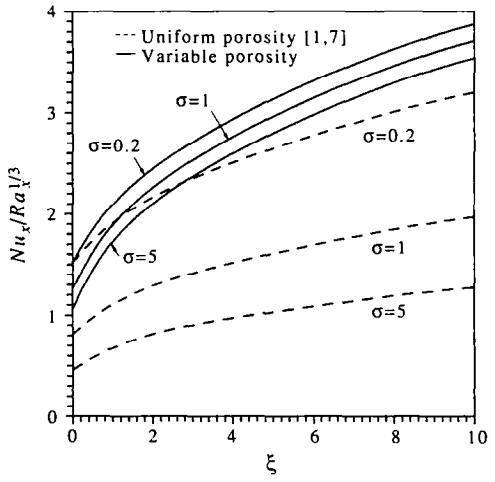

FIG. 4. Alternation of $Nu_x/Ra_x^{1/3}$ with ξ for various values of σ.

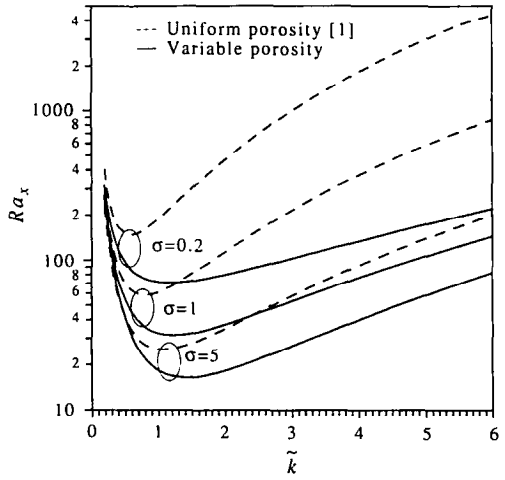

FIG. 5. Neutral stability curves for various values of σ with $\xi = 0$ (purely free convection).

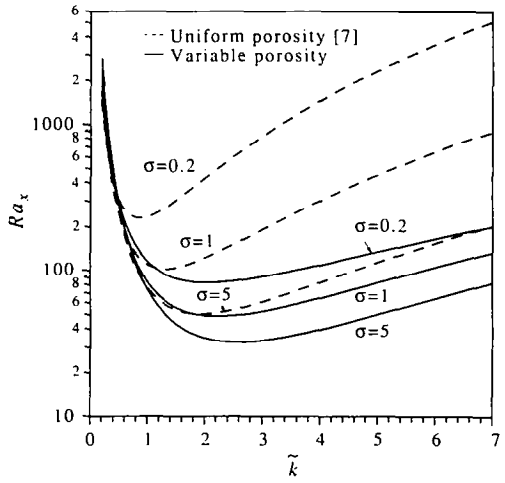

FIG. 6. Neutral stability curves for various values of σ with $\xi = 1$ (mixed convection).

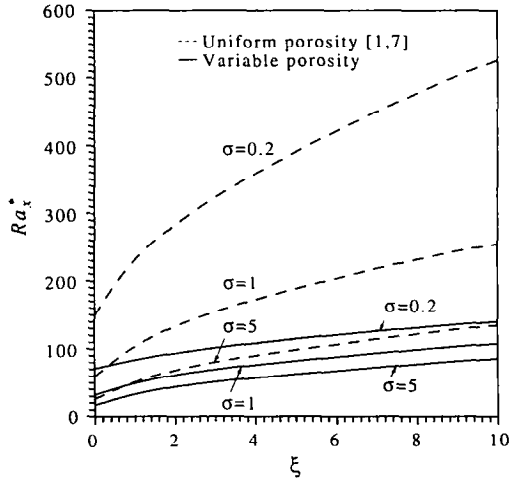

FIG. 7. Critical Rayleigh number as a function of ξ for various values of σ.

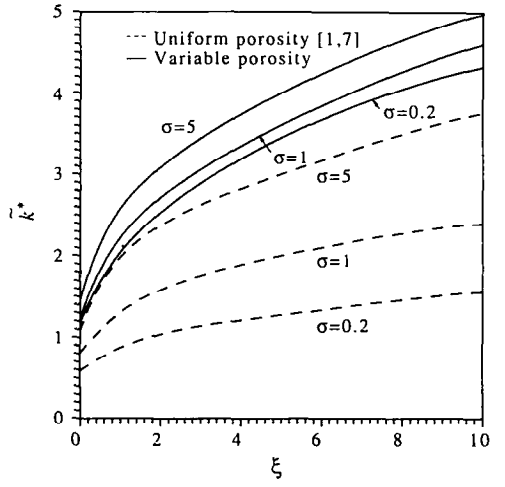

FIG. 8. Critical wave number as a function of ξ for various values of σ.

referred to the left and lower axes, while the temperature profiles are referred to the right and upper axes. The dashed lines represent the results for a uniform porosity medium while the solid lines are for a variable porosity medium. It should be noted that Darcy's law with uniform porosity [1, 7] corresponds to the case of $d = d^* = 0$. It is seen that the variable porosity effect increases the tangential velocity and reduces the thermal boundary layer thickness leading to an enhancement of heat transfer rate. Figure 4

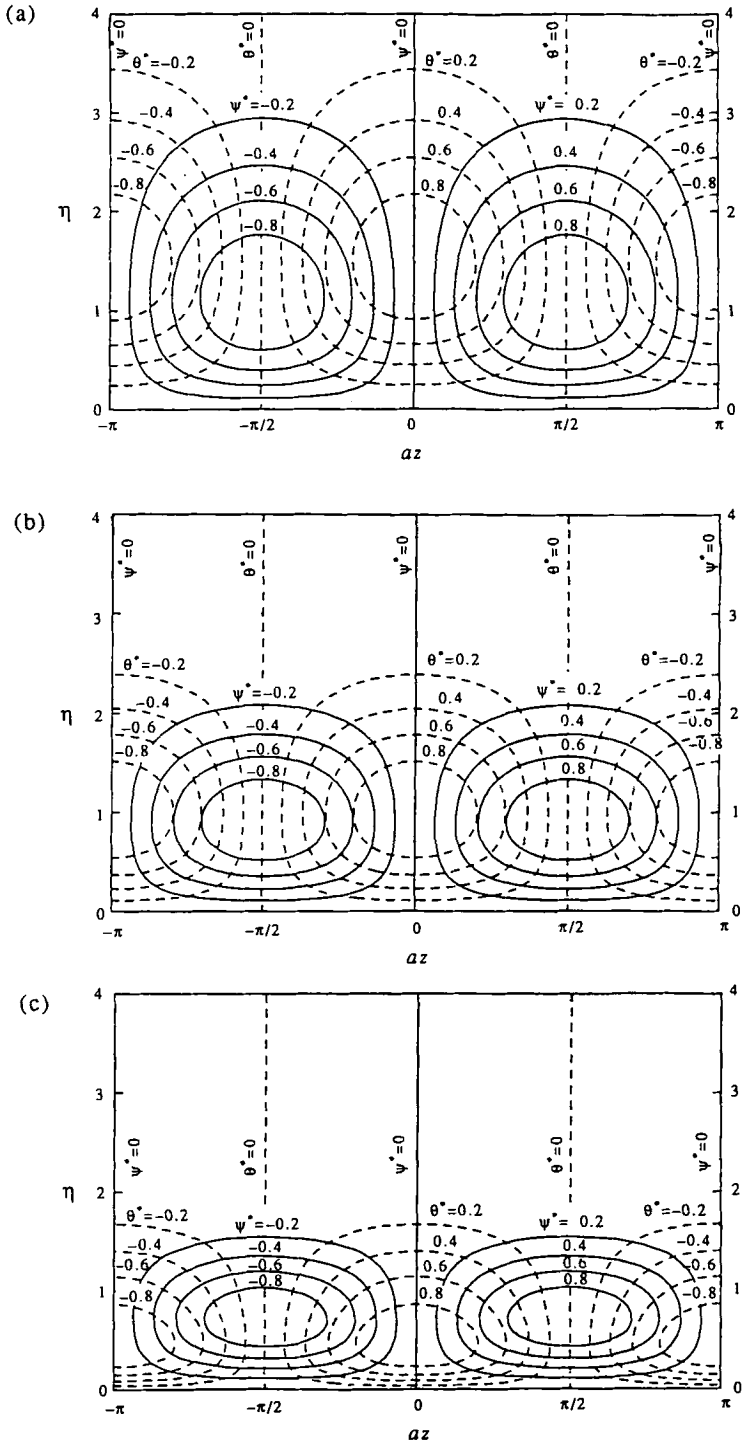

FIG. 9. The streamlines (solid lines) and isotherms (dashed lines) of the secondary flow at the onset of instability for uniform porosity media with $\xi = 1$ and (a) $\sigma = 0.2$, (b) $\sigma = 1$, (c) $\sigma = 5$.

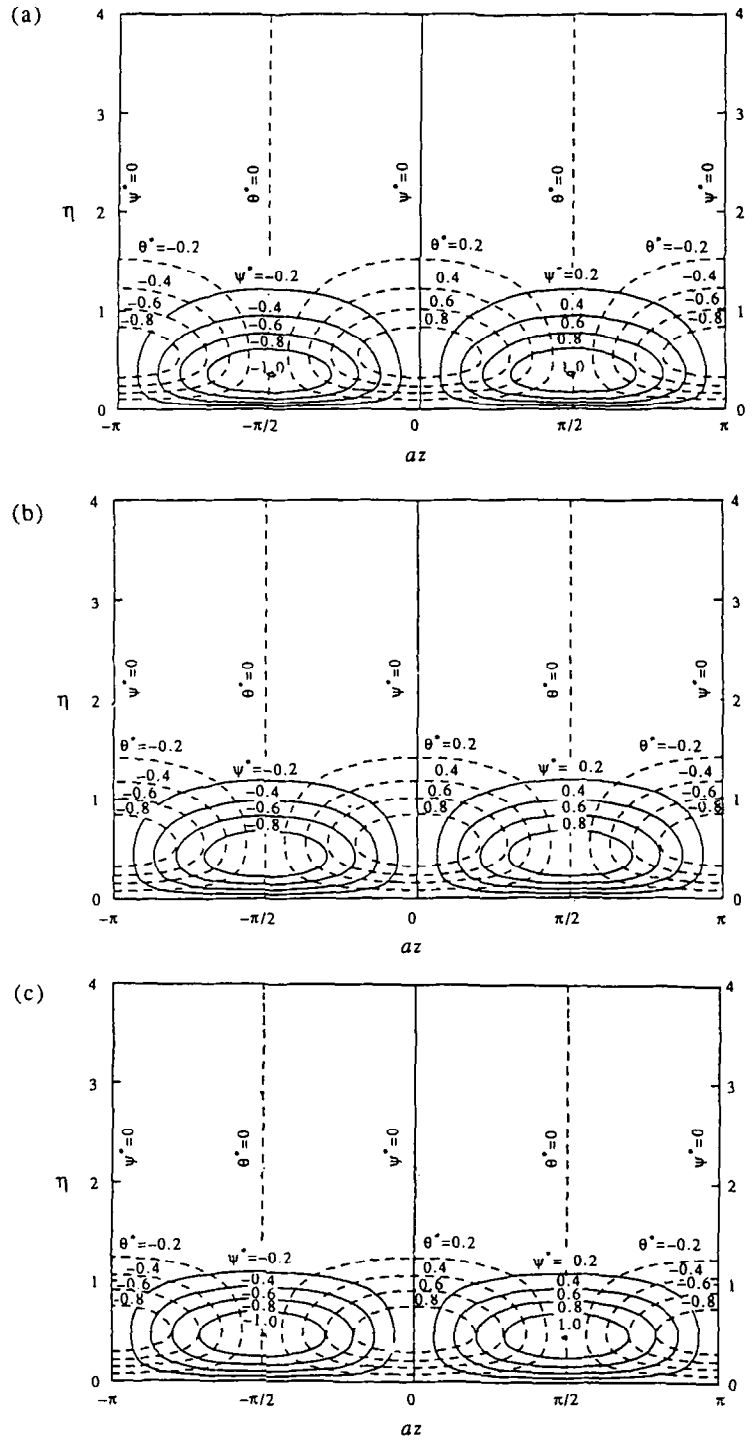

FIG. 10. The streamlines (solid lines) and isotherms (dashed lines) of the secondary flow at the onset of instability for variable porosity media with $\xi = 1$ and (a) $\sigma = 0.2$, (b) $\sigma = 1$, (c) $\sigma = 5$.

shows the alternation of Nusselt number with ξ for selected values of σ (0.2, 1 and 5). It follows from equation (20) that the effect of σ plays a role on the heat transfer rate not only through the temperature gradient at the wall but also through $\lambda_m(0)/\lambda_f$. Numerical results indicate that high conductivity of the solid phase (i.e. small values of σ) increases the heat transfer rate. It is also seen that, as would be expected, the variable porosity effect tends to increase the heat transfer rate.

Figures 5 and 6 show the neutral stability curves, in terms of the Rayleigh number Ra_x and the dimensionless wave number $\tilde{k}$, for selected values of σ (0.2, 1 and 5) for $\xi = 0$ (purely free convection) and $\xi = 1$, respectively. It is observed that as σ decreases, the neutral stability curves shift to higher Rayleigh number and lower wave number, indicating a stabilization of the flow to the vortex instability. Plotted with dashed lines in the figures for comparison are the neutral stability curves for uniform porosity media ($d = d^* = 0$) [1, 7]. It is seen that when the variable porosity effect is considered, the neutral stability curves shift to lower Rayleigh number and higher wave number, indicating a destabilization of the flow.

The critical Rayleigh number Ra_x^* and wave number $\tilde{k}^*$, which mark the onset of longitudinal vortices, can be found from the minima of the neutral stability curves. The critical Rayleigh number and wave number are plotted as function of ξ for selected values of σ in Figs. 7 and 8, respectively. Note that the case of Darcy's law with uniform porosity for a horizontal surface was considered by Hsu *et al.* [1] for a natural convection and by Hsu and Cheng [7] for a mixed convection. For $d = d^* = 0$, the present results are in good agreement with those of refs. [1, 7]. The results indicate that the variable porosity effect tends to destabilize the flow to the vortex mode of disturbance. It can also be seen that decreasing the value of σ would increase the critical Rayleigh number and stabilize the flow. Moreover, the larger the values of ξ, the more stable is the flow for the vortex instability. It is apparent from Fig. 8 that if either σ or ξ increases, the critical wave number $\tilde{k}^*$ increases. A close look at Figs. 7 and 8 indicates that the variable porosity effect is more pronounced as the mixed convection parameter ξ increases. For $\sigma = 0.2$ and $\xi = 0$ (natural convection), the critical Rayleigh number is reduced by about 52.2% relative to the uniform porosity result, while for $\xi = 10$ (mixed convection), the critical Rayleigh number is dramatically reduced by about 73.5%. Furthermore, one can see that the effects of thermal conductivity ratio σ on Ra_x^* and $\tilde{k}^*$ are more significant for a uniform porosity medium than for a variable porosity medium.

Figures 9 and 10 show the streamlines (solid lines) and isotherms (dashed lines) for the secondary flow at the onset of instability for uniform and variable porosity media, respectively, with three different values of σ (0.2, 1, 5) and $\xi = 1$. It is seen that as the fluid–solid thermal conductivity ratio σ increases, the size of the vortex roll decreases resulting in high dense streamlines near the wall. It is noted that this trend is more apparent for a uniform porosity medium (Fig. 9) than for a variable porosity medium (Fig. 10). By comparing Fig. 9 with Fig. 10, it shows a relatively high density of streamlines near the heated wall for a variable porosity medium. This implies that for a variable porosity medium the fluid near the heated wall moves relatively fast when compared with a uniform porosity medium. Consequently, for a variable porosity medium, this fast moving fluid near the heated wall convects relatively more energy away thus causing a larger temperature gradient and making the flow more susceptible for the vortex mode of instability.

5. CONCLUSIONS

The effects of variable porosity and fluid–solid thermal conductivity ratio σ to the vortex instability of horizontal mixed convection boundary layer flow in saturated porous medium have been examined by a linear stability theory. The numerical results demonstrate that the variable porosity effect tends to enhance the heat transfer rate and destabilize the flow. As the fluid–solid thermal conductivity ratio decreases, both the Nusselt number and critical Rayleigh number increase and the flow is more stable for the vortex mode of disturbance. It is also shown that the variable porosity effect is more pronounced as the mixed convection parameter ξ increases. Moreover, the effects of fluid–solid thermal conductivity ratio on the Nusselt number, critical Rayleigh and wave numbers are more significant for a uniform porosity medium than for a variable porosity medium. It should be noted that when the channeling effect due to the variable porosity is considered, it will usually be necessary to also account for the boundary viscous friction effect. Unlike the variable porosity effect, the boundary effect is shown to stabilize the flow [16]. Thus, the boundary effect should be incorporated in the future analysis. The combined effects of variable porosity and boundary friction on the vortex instability is currently under investigation by the authors.

REFERENCES

1. C. T. Hsu, P. Cheng and G. M. Homsy, Instability of free convection flow over a horizontal impermeable surface in a porous medium, *Int. J. Heat Mass Transfer* **21**, 1221–1228 (1978).
2. C. T. Hsu and P. Cheng, Vortex instability in buoyancy-induced flow over inclined heated surfaces in a porous medium, *J. Heat Transfer* **101**, 660–665 (1979).
3. J. Y. Jang and W. J. Chang, Vortex instability of buoyancy-induced inclined boundary layer flow in a saturated porous medium, *Int. J. Heat Mass Transfer* **31**, 759–767 (1988).
4. J. Y. Jang and W. J. Chang, The flow and vortex instability of horizontal natural convection in a porous medium resulting from combined heat and mass buoyancy effects, *Int. J. Heat Mass Transfer* **31**, 769–777 (1988).
5. J. Y. Jang and W. J. Chang, Vortex instability of inclined buoyant layer in porous media saturated with cold water, *Int. Commun. Heat Mass Transfer* **14**, 405–416 (1987).
6. J. Y. Jang and W. J. Chang, Maximum density effects on vortex instability of horizontal and inclined buoyancy induced flows in porous media, *J. Heat Transfer* **111**, 572–574 (1989).
7. C. T. Hsu and P. Cheng, Vortex instability of mixed convective flow in a semi-infinite porous medium bounded by a horizontal surface, *Int. J. Heat Mass Transfer* **23**, 789–798 (1980).

8. P. Cheng, Combined free and forced convection flow about inclined surfaces in porous media, *Int. J. Heat Mass Transfer* **20,** 807–814 (1977).
9. C. T. Hsu and P. Cheng, The onset of longitudinal vortices in mixed convective flow over an inclined surface in a porous medium, *J. Heat Transfer* **102,** 544–549 (1980).
10. J. Y. Jang and K. N. Lie, Vortex instability of mixed convection flow over horizontal and inclined surfaces in a porous medium, *Int. J. Heat Mass Transfer* **35,** 2077–2085 (1992).
11. K. Vafai, Convective flow and heat transfer in variable-porosity media, *J. Fluid Mech.* **147,** 233–259 (1984).
12. B. C. Chandrasekhara, P. M. S. Namboodiri and A. R. Hanumanthappa, Similarity solutions for buoyancy induced flow in a saturated porous medium adjacent to impermeable horizontal surface, *Wärme- und Stoffübertragung* **18,** 17–23 (1984).
13. B. C. Chandrasekhara, Mixed convection in the presence of horizontal impermeable surfaces in saturated porous media with variable permeability, *Wärme- und Stoffübertragung* **19,** 195–201 (1985).
14. B. C. Chandrasekhara and P. M. S. Namboodiri, Influence of variable permeability on combined free and forced convection about inclined surfaces in porous media, *Int. J. Heat Mass Transfer* **28,** 199–206 (1985).
15. J. T. Hong, Y. Yamada and C. L. Tien, Effects of non-Darcian and nonuniform porosity on vertical-plate natural convection in porous media, *J. Heat Transfer* **109,** 356–362 (1987).
16. W. J. Chang and J. Y. Jang, Non-Darcian effects flow in a porous medium, *Int. J. Heat Mass Transfer* **32,** 529–539 (1989).
17. W. J. Chang and J. Y. Jang, Inertia effects on vortex instability of a horizontal natural convection flow in a saturated porous medium, *Int. J. Heat Mass Transfer* **32,** 541–550 (1989).
18. J. Y. Jang and J. L. Chen, Thermal dispersion and inertia effects on vortex instability of a horizontal mixed convection flow in a saturated porous medium, *Int. J. Heat Mass Transfer* **36,** 383–389 (1993).
19. A. R. Wazzan, T. T. Okamura and H. M. O. Smith, Stability of laminar boundary layer at separation, *Physics Fluids* **10,** 2540–2545 (1967).
20. P. Zehner and E. U. Schlünder, Waermeleleitfahigkeit von Schuettungen bei massigen Temperaturen, *Chemie-Ingr-Tech.* **42,** 993–941 (1970).